OXFORD SIMB Society for Industrial Microbiology and Biotechnology

Journal of Industrial Microbiology and Biotechnology, 2023, 50, kuad029

https://doi.org/10.1093/jimb/kuad029

Advance access publication date: 13 September 2023

Bioenergy/Biofuels/Biochemicals – Original Paper

Co-feeding enhances the yield of methyl ketones

Anita L. Ziegler [1,†], Carolin Grütering [2,3,†], Leon Poduschnick[1,2], Alexander Mitsos [4,1,5], Lars M. Blank [2]

[1]Process Systems Engineering (AVT.SVT), RWTH Aachen University, 52074 Aachen, Germany
[2]Institute of Applied Microbiology (iAMB), RWTH Aachen University, 52074 Aachen, Germany
[3]Bioeconomy Science Center (BioSC), Forschungszentrum Jülich GmbH, 52428 Jülich, Germany
[4]JARA-ENERGY, 52056 Aachen, Germany
[5]Institute of Energy and Climate Research: Energy Systems Engineering (IEK-10), Forschungszentrum Jülich GmbH, 52425 Jülich, Germany.
Correspondence should be addressed to: Lars M. Blank, Institute of Applied Microbiology (iAMB), RWTH Aachen University, 52074 Aachen, Germany.
E-mail: lars.blank@rwth-aachen.de
[†]Equally contributing authors.

Abstract: The biotechnological production of methyl ketones is a sustainable alternative to fossil-derived chemical production. To date, the best host for microbial production of methyl ketones is a genetically engineered *Pseudomonas taiwanensis* VLB120 Δ6 pProd strain, achieving yields of 101 mgg^{-1} on glucose in batch cultivations. For competitiveness with the petrochemical production pathway, however, higher yields are necessary. Co-feeding can improve the yield by fitting the carbon-to-energy ratio to the organism and the target product. In this work, we developed co-feeding strategies for *P. taiwanensis* VLB120 Δ6 pProd by combined metabolic modeling and experimental work. In a first step, we conducted flux balance analysis with an expanded genome-scale metabolic model of iJN1463 and found ethanol as the most promising among five cosubstrates. Next, we performed cultivations with ethanol and found the highest reported yield in batch production of methyl ketones with *P. taiwanensis* VLB120 to date, namely, 154 mg g^{-1} methyl ketones. However, ethanol is toxic to the cell, which reflects in a lower substrate consumption and lower product concentrations when compared to production on glucose. Hence, we propose cofeeding ethanol with glucose and find that, indeed, higher concentrations than in ethanol-fed cultivation (0.84 g L_{aq}^{-1} with glucose and ethanol as opposed to 0.48 g L_{aq}^{-1} with only ethanol) were achieved, with a yield of 85 mg g^{-1}. In a last step, comparing experimental with computational results suggested the potential for improving the methyl ketone yield by fed-batch cultivation, in which cell growth and methyl ketone production are separated into two phases employing optimal ethanol to glucose ratios.

One-Sentence Summary: By combining computational and experimental work, we demonstrate that feeding ethanol in addition to glucose improves the yield of biotechnologically produced methyl ketones.

Keywords: Methyl ketones, Co-feeding, *Pseudomonas*, Constraint-based modeling

Graphical abstract

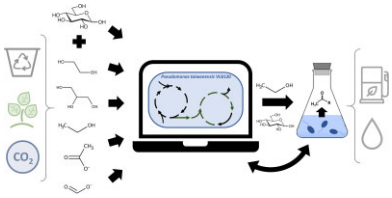

Workflow for *in silico* and experimentally guided co-feeding strategies.

Introduction

Methyl ketones are a versatile class of platform chemicals that are currently produced by the oxidation of hydrocarbons. Aliphatic, medium-chain-length methyl ketones are used in the flavor and fragrance industry (Goh et al., 2012).

In the last decade, applications for sustainable production of lubricants (Balakrishnan et al., 2016) and diesel fuel replacements (Harrison & Harvey, 2018) have been discussed. In order to provide a sustainable route for methyl ketone production, extensive research has been carried out to enable microbial production from renewable resources. A first recombinant pathway for the production of medium-chain-length methyl ketones (C12–C15), as diesel replacement, was introduced by Goh et al. (2012) in *Escherichia coli* strain DH1. The genetic engineering efforts that particularly involved altering the fatty acid metabolism led to the overproduction of saturated and monounsaturated methyl ketones with a chain length of C11–C15 at a titer of 0.38 g L^{-1}. Since then, methyl ketone production has been achieved in various Gram-negative microorganisms such as *Cupriavidus necator* and *Pseudomonas putida* by means of genetic engineering (Dong et al., 2019; Müller et al., 2013). Gram-negative *Pseudomonas taiwanensis* VLB120 has many characteristics that make it interesting for

Received: April 12, 2023. **Accepted:** September 11, 2023.

industrial application in bioprocesses. They are nonpathogenic, show high tolerance to organic solvents, can utilize a broad variety of substrates, and are easily genetically engineered. Additionally, *P. taiwanensis* VLB120 shows a high tolerance to lignin-derived aromatic compounds that have an inhibitory effect on many other microorganisms (Lenzen et al., 2019; Wordofa & Kristensen, 2018). Nies et al. (2020) engineered *P. taiwanensis* VLB120 for the production of medium-chain-length methyl ketones. They established the truncated β-oxidation pathway from Goh et al. (2012) to Goh et al. (2014). The strain *P. taiwanensis* VLB120 Δ6 pProd additionally had deletions of *fadA2*, *tesB*, and the *pha* operon. In a fed-batch bioprocess with glucose as a carbon source, a product titer of 9.8 g L_{aq}^{-1} at 53% of the theoretical maximum yield was achieved. This is the highest recombinantly produced methyl ketone yield to date (Nies et al., 2020).

Independent of the microorganism, strategies for methyl ketone production aim for increased availability of fatty acid precursors malonyl-CoA and acetyl-CoA (AcCoA) or the improvement of the conversion rate of fatty acids in the beta-oxidation pathway. Increased availability of ATP and NAD(P)H was shown to have a positive impact as well, since the fatty acid metabolism in general has a high demand for energy carriers and redox cofactors (Hollinshead et al., 2014). In order to be competitive with the petrochemical industry, high methyl ketone yields are required when applying microbial production hosts. Similarly, to other fatty acid-derived products, the main challenge is the high demand for ATP along with a complex redox balancing. Herein, the difficulty lies in a net NADH consumption and a net NADPH production (Goh et al., 2018; Hollinshead et al., 2014). Often, these challenges are tackled by means of genetic engineering; however, redox balancing can be cumbersome (Zu et al., 2021).

An alternative strategy to improve product formation is the choice of substrate. The utilized carbon source is a lever to rearrange the metabolic fluxes and improve product yields independent of genetic engineering. Different substrates are metabolized by different metabolic pathways, resulting in specific carbon-to-energy ratios. The application of multiple carbon sources in a co-feeding approach has been shown to be advantageous in several applications (Dong et al., 2019; Ullmann et al., 2021). Especially for the production of highly reduced products such as methyl ketones, co-feeding was beneficial (Park et al., 2019). Also, from an ecological perspective, the use of additional, alternative carbon sources can be beneficial. For example, ethanol can be produced from greenhouse gases in syngas fermentations and from formate by electrochemical reduction of CO_2 (Bengelsdorf & Dürre, 2017; Cotton et al., 2020). *Pseudomonas spp.* are described as being able to metabolize a broad variety of carbon sources, including pentose and hexose sugars, carboxylic acids, and aromatic compounds (Lang et al., 2014; Sivapuratharasan et al., 2022; Sudarsan et al., 2014; Wordofa & Kristensen, 2018). We have preselected five different potential carbon sources as a potential cofeeding compound. Glycerol, ethylene glycol, ethanol, acetate, and formate were chosen because it was previously demonstrated that these substances can have a positive impact on a bioprocess when they are used as a (co-)substrate. Additionally, all applied co-substrates can either be derived from industrial side streams (glycerol, ethylene glycol) or from sustainable resources such as lignocellulosic biomass or CO_2 (ethanol, acetate, and formate) (Li et al., 2019; Nikel & de Lorenzo, 2014; Sun et al., 2020; Ullmann et al., 2021; Xu et al., 2021).

When evaluating co-substrates, metabolic modeling is a powerful tool to support and reduce the effort of laboratory experiments. Metabolic modeling is based on genome-scale metabolic models (GEMs), which are reconstructions of metabolic networks, that is, of all reaction pathways existing in an organism. GEMs contain the stoichiometry of the reactions as well as their associated genes. GEMs serve to predict the phenotypical response of an organism to different environmental conditions, for example, when co-feeding, as well as to predict the inner-cellular fluxes by applying metabolic modeling formulations, such as flux balance analysis (FBA) (Orth et al., 2010; Varma & Palsson, 1994). With the assumption of steady-state, FBA defines a cellular objective and additional constraints on the reaction fluxes and calculates the resulting flux distribution by means of linear programming.

Herein, we applied FBA to preassess which co-substrate is the most promising candidate to improve the yield of methyl ketones. Next, we conducted growth experiments with *P. taiwanensis* VLB120 Δ6 pProd on the most promising substrate to measure the product titer and yield under different cofeeding conditions. With these experimental results, we redid the FBA prediction with the experimental uptake rates as input to furnish consistent results and compute potentials for further improvement of the methyl ketone yield. To conclude, we used metabolic modeling to reduce laboratory work to develop the co-feeding strategies for improved methyl ketone yield.

Materials and Methods

Strains, Media, and Culture Conditions

The chemicals used in this work were obtained from Carl Roth (Karlsruhe, Germany), Sigma-Aldrich (St. Louis, MO, USA), or Merck (Darmstadt, Germany) unless stated otherwise. *P. taiwanensis* Δ6 pProd was propagated in Lysogeny Broth (LB) containing 10 g L^{-1} peptone, 5 g L^{-1} sodium chloride, and 5 g L^{-1} yeast extract. Solid LB was prepared by adding 1.5% (w/v) agar to the liquid medium. Gentamycin and kanamycin were added at concentrations of 25 m gL^{-1} and 50 m gL^{-1}, respectively. Main cultures for biomass formation and methyl ketone production were performed in 500 mL shake flasks with 10% (v/v) of mineral salt medium (MSM; Hartmans et al., 1989) with 7.76 g L^{-1} K_2HPO_4, 3.26 g L^{-1} NaH_2PO_4, 2.0 g L^{-1} (NH_4 $2SO_4$), 0.1 g L^{-1} $MgCl_2 \cdot 6\ H_2O$, 10.0 mg L^{-1} EDTA, 2.0 mg L^{-1} $ZnSO_4 \cdot 7\ H_2O$, 1.0 mg L^{-1} $CaCl_2 \cdot 2\ H_2O$, 5.0 mg L^{-1} $FeSO_4 \cdot 7\ H_2O$, 0.2 mg L^{-1} $Na_2MoO_4 \cdot 2\ H_2O$, 0.2 mg L^{-1} $CuSO_4 \cdot 5\ H_2O$, 0.4 mg L^{-1} $CoCl_2 \cdot 6\ H_2O$ and 1.0 mg L^{-1} $MnCl_2 \cdot 2\ H_2O$ supplemented with the respective carbon source and antibiotics. In contrast to the standard MSM medium, the concentration of the phosphate buffer was doubled in order to minimize the drop of the pH value that can occur due to gluconate production. All cultivations were performed at 30°C, and shaken cultures had a shaking diameter of 50 mm. Before inoculation of the preculture, frozen glycerol stocks were streaked on LB agar plates with antibiotics and incubated for 24 hr. Next, 5 mL of LB media with antibiotics were inoculated from a single colony in a 15 mL glass tube and cultivated overnight at 200 min^{-1}. The second preculture was performed in MSM with 10 g L^{-1} glucose in a 500-mL shake flask and a filling volume of 10% at 300 min^{-1}. This preculture was inoculated to an optical density at 600 nm (OD_{600}) of 0.1 in mineral salt media until the late exponential phase for inoculation of the main culture. The starting OD_{600} of main cultures was 0.1–0.3. Main cultures in shake flasks were performed in 500-mL shake flasks at 300 min^{-1} using MSM with the respective carbon source and a filling volume of 10%. In the case of methyl ketone production, 1 mM arabinose and 2 mM isopropyl β-D-1-thiogalactopyranoside (IPTG) were added before inoculation to induce product formation, and 12.5 mL of *n*-decane were added for *in situ* product extraction. For online measurement of scattered light during growth in 96-

well microtiter plates (MTPs), the BioLector (Beckman Coulter Life Sciences, USA) was used. Each experimental condition had three additional blank wells without microorganisms to determine the baseline signal for light scattering. The scattered light signal was measured with a gain of 30 and 50 at a wavelength of 620 nm. The measurement interval was set to 13 min. The temperature was set to 30°C, and the humidity was kept at 85%. The culture was shaken at 900 min^{-1} with a shaking diameter of 3 mm.

Analysis of Cell Growth, Carbon Sources, and Product Formation

Biomass concentration of *P. taiwanensis* Δ6 pProd was measured in aqueous phases and determined as cell dry weight (CDW) in predried glass vials and (OD_{600}) values. Prior to the cultivations, the correlation of these two units was measured. In the case that only the (OD_{600}) value was measured using an Ultrospec™ 10 Cell Density Meter (Harvard Bioscience, Holliston, MA, USA), CDW values were determined by

$$\mathrm{CDW}\left[\mathrm{g\,L^{-1}}\right] = 0.44\,\mathrm{OD_{600}}.$$

Aqueous phases were centrifuged for 120 s at 13 000 min^{-1}, filtered through a 0.2 µm membrane, and stored at −20°C until further high-pressure liquid chromatography (HPLC-UV-RI) analysis. Supernatants were analyzed in a DIONEX UltiMate 3000 HPLC System (Thermo Scientific, Waltham, MA, USA) with a Metab-AAC column (300 × 7.8 mm column, ISERA). Elution was performed with 5 mM H_2SO_4 at a flow rate of 0.6 mL min^{-1} and a column temperature of 40°C. For detection, a SHODEX RI-101 detector (Showa Denko Europe GmbH, Munich, Germany) and a DIONEX UltiMate 3000 Variable Wavelength Detector set to 210 nm were used. The substrates were identified and quantified via retention time and UV/RI quotient compared to corresponding external standards. In the case that an organic phase was present for *in situ* extraction of methyl ketones, the phases were separated by centrifugation for 120 s at 13 000 min^{-1}. Analysis of methyl ketones in the organic phase was performed using a Trace GC Ultra (Thermo Scientific, Waltham, MA, USA) gas chromatography with a flame ionization detector (FID) and a polar ZB-WAX column (30 m length, 0.25 mm inner diameter, and 0.25 µm film thickness, Zebron, Phenomenex, UK). The measurements were performed at a constant helium flow rate of 2 mL min^{-1} and a split ratio of 1:10. The initial oven temperature of 80°C was held for 2.5 min, increased to 250°C at 20°C min^{-1}, and then held constant at 250°C for 10 min. The injector temperature was set to 250°C and the injection volume was 1 µL, while the temperature of the FID was 290°C. Methyl ketones were quantified using external standards of 2-undecanone, 2-tridecanone, 2-pentadecanone, and 2-heptadecanone (Tokyo Chemical Industry Co., Tokyo, Japan). In the case of simultaneous measurement of CDW and product concentration, six equal shake flasks were run under the same conditions. This was necessary since the *n*-decane overlay hinders reproducible biomass quantification due to emulsion formation. Three shake flasks had an overlay of *n*-decane for methyl ketone measurement, while three shake flasks did not include an organic phase and were used for CDW quantification.

Degree of Reduction

The degree of reduction (DoR) describes the number of electrons that can be derived from the complete oxidation of a specific molecule. The DoR can be used as an estimate of the energy that is yielded from a carbon substrate by microorganisms. A higher DoR corresponds to a more highly reduced compound, from which more redox cofactors can be produced and, thus, more energy can be generated. It is determined by Stephanopoulos et al. (1998) and Heijnen and Roels (1981):

$$\begin{aligned} &\mathrm{C_aH_bO_c} \\ &DoR = \frac{4\cdot a + 1\cdot b - 2\cdot c}{a}, \end{aligned} \tag{1}$$

where *a*, *b*, and *c* are the number of C-atoms, H-atoms, and O-atoms, respectively.

GEM of *P. taiwanensis* Δ6 Pprod

For the reconstruction of the metabolic network of *P. taiwanensis* VLB120 Δ6 pProd, the most current and complete network of the closely related organism *P. putida* KT2440 was used, that is, iJN1463 (Nogales et al., 2020). The network iJN1463 contains 2 153 metabolites, 2 927 reactions, and 1 463 genes. Herein, the network iJN1463 was adjusted mainly according to the modifications introduced by Nies et al. (2020). In their GEM for *P. taiwanensis* VLB120, named iJN1411_MK, they took the metabolic network reconstruction iJN1411 for *P. putida* KT2440 (Nogales et al., 2017) as a basis. They adapted iJN1411 by removing and adding reactions and metabolites to switch from *P. putida* to *P. taiwanensis* VLB120. The GEM iJN1463 was modified according to iJN1411_MK, with the following differences: The reactions DABAAT2 and AHSERL2 were not relevant for biomass production in iJN1411 but are relevant for biomass production in iJN1463 and were therefore not deleted. Moreover, the reaction SHSL2r instead of SHSL2 was deleted because SHSL2 does not exist in iJN1463.

In the model iJN1411_MK, Nies et al. (2020) added a methyl ketone pooling reaction for methyl ketone congeners. Contrary to their suggestion, in this work, we accounted for the C17-congener 10-heptadecen-2-one. The new pooling reaction reads:

$$\begin{aligned} &1.00\ \cdot\ \text{2-pentadecanone\_e} + 14.92\ \cdot\ \text{8-pentadecen-2-one\_e} \\ &+1.34\ \cdot\ \text{10-heptadecen2-one\_e} + 15.46 \\ &\cdot\text{2-tridecanone\_e} + \ 24.04\ \cdot\ \text{6-tridecen-2-one\_e} \\ &+ 20.08\ \cdot\ \text{2-undecanone\_e} \rightarrow, \end{aligned}$$

where e indicates that the metabolites are extracellular and where the stoichiometry corresponds to the molar ratio of the methyl ketone congeners that was determined experimentally by Nies et al. (2020). Note that, as the reaction is a so-called exchange reaction, only reactants and no products are assigned to this reaction. Additionally, two reactions, that is, one producing 2-undecanone and one transporting 2-undecanone to the extracellular space, were added in alignment with the other congener reactions. With the aforementioned adaptations implemented, the adapted GEM was named iJN1463_MK.

The genetically modified strain Δ6 pProd was implemented in the model according to Nies et al. (2020) by constraining the corresponding reactions in the GEM iJN1463_MK to zero. An overview of the genes can be found in Supplementary Section A1. Knocking out the genes *fadE* and *fadE2*, however, made the production of methyl ketones computationally impossible as certain metabolites that are important for the production of methyl ketones could not be synthesized anymore. The reason for this is that the gene *co_aco* is not implemented in iJN1463_MK but is present in the mutant strain. The gene *co_aco* originates from *M. luteus* and encodes the enzyme acyl-CoA dehydrogenase that catalyzes the synthesis of the needed metabolite, just as *fadE* and *fadE2*, but with

different reaction partners. Equation (2) shows the reaction originating from the genes *fadE* and *fadE2*, while Equation (3) shows the heterologous equivalent from *M. luteus* with the gene *co_aco*.

$$\text{acyl-CoA} + \text{FAD} \rightleftharpoons \text{trans-2, 3-dehydroaycl-CoA} + \text{FADH}_2, \quad (2)$$

$$\text{acyl-CoA} + O_2 \rightleftharpoons \text{trans-2, 3-dehydroacyl-CoA} + H_2O_2. \quad (3)$$

All 35 reactions catalyzed by acyl-CoA dehydrogenase were adjusted in the metabolic network such that FAD and $FADH_2$ were replaced with O_2 and H_2O_2, respectively. With the knockouts implemented, we refer to the modulated network as iJN1463_MK Δ6 pProd in the following. All adaptations in this section were conducted in Python™ version 3.9.12, and iJN1463_MK Δ6 pProd is openly available at Ziegler et al. (2023).

Flux Balance Analysis

FBA is mathematically formulated as a linear optimization program:

$$\max_{\boldsymbol{v}\in\mathbb{R}^n} \boldsymbol{c}^T\boldsymbol{v}$$
$$\text{s.t. } \boldsymbol{S}\,\boldsymbol{v} = 0$$
$$v_i^{lb} \le v_i \le v_i^{ub}\ \forall\, i \in \{1, \ldots, n\},$$

where $\boldsymbol{v}$ is the vector of reaction fluxes, n is the number of reactions in the GEM, and $\boldsymbol{c}$ is a parameter vector that indicates which reaction flux shall be optimized in the objective function. The matrix $\boldsymbol{S}$ denotes the stoichiometric matrix of the GEM, and the equality constraint ensures a closed mass balance, corresponding to the assumption of steady-state. The parameters v_i^{lb} and v_i^{ub} impose lower and upper bounds on the fluxes, respectively, with $v_i^{lb} \ge 0$. In this work, the maximization of the methyl ketone exchange reaction, or the biomass exchange reaction BIOMASS_KT2440_WT3 was chosen as cellular objective. The lower bound on the adenosine triphosphate maintenance (ATPM) reaction, which corresponds to the nongrowth-associated ATP maintenance requirement (NGAM), was set to 0.52 mmol g_{CDW}^{-1} hr^{-1} (Nies et al., 2020), according to experimental data from Ebert et al. (2011). The computations were performed using the software COBRApy (Ebrahim et al., 2013) and the optimization software Gurobi 9.5.1 (Gurobi Optimization, LLC, 2023). For comparison of experimental results with computational results, time-resolved concentrations from HPLC UV RI measurements in the exponential growth phase were used to calculate flux rates (Chmiel et al., 2018; Varma & Palsson, 1994). The conversion equations can be found in the Supplementary Information. The code for the FBA computations is openly available at Ziegler et al. (2023).

Results and Discussion

Case Study: Metabolic Modeling Detects Ethanol as the Most Promising Co-Substrate

To represent co-feeding, different uptake fluxes were set as inputs to the FBA. Within a range of 0 C-mmol/g_{CDW}/hr to 18 C-mmol/g_{CDW}/hr, the substrate was varied as glucose plus each denominated co-substrate. The 18 C-mmol/g_{CDW}/hr corresponds to 3 mmol g_{CDW}^{-1} hr^{-1} glucose, in alignment with the experimentally measured uptake rate by Nies et al. (2020). Each input square was covered by 20 times 20 FBA predictions. The methyl ketone exchange reaction flux was maximized to calculate the maximal theoretical methyl ketone production. The resulting ranking of substrates indicates the performance of the substrates, implicitly assuming that the actual production is proportional to the maximal theoretical production. Each FBA is subject to 10% of the maximal theoretical biomass at the respective point, representing the standard growth maintenance. In this parametric linear optimization program, the input space can be seen as a square and the results form planes, as seen in Fig. 1. No kinks are visible, which means that the optimal basis does not change but rather the active reaction pathways within the metabolic network stay the same.

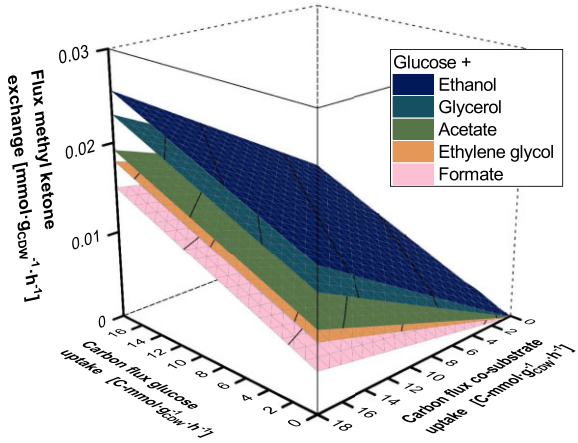

Fig. 1. Evaluation of five co-substrates using flux balance analysis as a function of glucose and co-substrate carbon uptake. The methyl ketone exchange reaction flux was set as objective function. This exchange reaction is normalized for 2-pentadecanone. A threshold on biomass of 10% of the maximal theoretical growth at each point was imposed.

Table 1. Degree of Reduction (DoR) for Glucose and Five Co-Substrates, Calculated Using Equation (1)

Name	Chemical formula	DoR
Ethanol	C_2H_6O	6
Ethylene glycol	$C_2H_6O_2$	5
Glycerol	$C_3H_8O_3$	4.67
Glucose	$C_6H_{12}O_6$	4
Acetate	$C_2H_4O_2$	4
Formate	CH_2O_2	2

Figure 1 shows that the highest methyl ketone flux of 0.026 mmol g_{CDW}^{-1} hr^{-1} is reached with the co-substrate ethanol and at maximal glucose and ethanol input. The second-best-performing co-substrate is glycerol, followed by acetate and ethylene glycol. With the co-substrate formate, the maximum reachable methyl ketone flux is 0.015 mmol g_{CDW}^{-1} hr^{-1}.

The slope of the planes corresponds to the yield of methyl ketones. When only varying glucose, the yield stays constant at 0.67 mmol C-mol^{-1} for all co-substrates, which was to be expected. When varying the co-substrate, the steepest descent is visible with ethanol, which achieves a yield of 0.85 mmol C-mol^{-1}, which is higher than the yield on glucose. In other words, more carbon atoms are required with glucose as a carbon source to form the same amount of methyl ketones than on ethanol. Similarly, glycerol exhibits a higher yield than pure glucose, whereas the other co-substrates have a lower yield than pure glucose.

The results from Fig. 1 were compared to the DoR of glucose and the five co-substrates. Table 1 displays the DoR calculated with Equation (1).

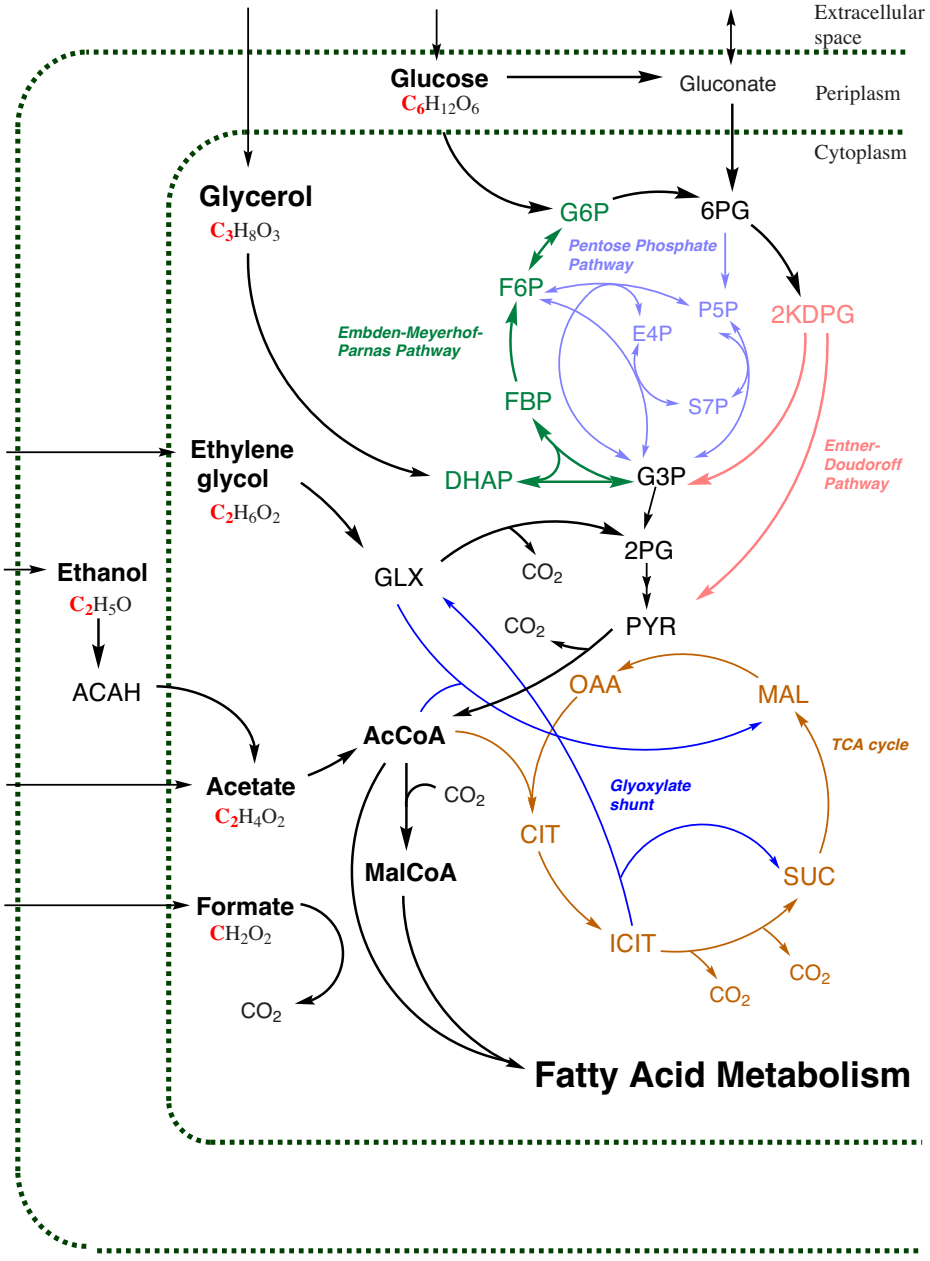

Fig. 2. Simplified central carbon metabolism of *P. taiwanensis* VLB120 with focus on the utilization pathways of glucose, glycerol, ethylene glycol, ethanol, acetate, and formate, as suggested by Li et al. (2019), Tiso et al. (2021), Yang et al. (2019), Poblete-Castro et al. (2020), and Zobel et al. (2017). The map was created with ChemDraw 21.0.0. G6P = glucose 6-phosphate; 6PG = 6-phospho gluconate; 2KDPG = 2-keto-3-desoxyphosphogluconate; F6P = fructose 6-phosphate; FBP = fructose 1,6-bisphosphate; G3P = glycerinaldehyde 3-phosphate; DHAP = dihydroxyacetone phosphate; E4P = erythrose 4-phosphate; P5P = 5-phosphate pentoses; S7P = seduheptolose 7-phosphate; 2PG = 2-phospho glycerate; PYR = pyruvate; GLX = glyoxylate; AcCoA = acetyl-CoA; ACAH = acetaldehyde; MalCoA = malonyl-CoA; OAA = oxalacetate; CIT = citrate; ICIT = isocitrate; SUC = succinate; MAL = malate.

The DoR is a first estimation of how many electrons the microorganism can derive from a certain substrate. The higher the DoR, the more energy the substrate carries. Interestingly, the DoR displays a different order compared to the aforementioned FBA results. Namely, the DoR suggests that ethylene glycol should perform better than it did in the FBA. Moreover, the DoR indicates that acetate should perform as good as pure glucose.

To further understand the differences, the metabolism of the different substrates was investigated in the literature. Figure 2 shows the main metabolization pathways of glucose and the five co-substrates in a metabolic map.

The metabolization of glucose to glucose 6-phosphate goes along with the investment of one ATP molecule. Glycerol is converted to dihydroxyacetone phosphate (DHAP; Poblete-Castro et al., 2020), which further goes into the Embden–Meyerhof–Parnas pathway. Ethylene glycol is transformed into glyoxylate (GLX). GLX can further be transformed via the GLX shunt, producing $2CO_2$ and redox cofactors. Alternatively, GLX can be converted to tatronate semialdehyde and CO_2, and further to pyruvate. Hence, in this pathway, a lot of carbon is lost. The first option makes ethylene glycol an energy carrier rather than a carbon source, while in the second option, it is an inefficient carbon

source (Li et al., 2019; Tiso et al., 2021). Ethanol is metabolized via acetaldehyde (ACAH) and acetate to AcCoA without carbon losses, that is, CO_2 production (Bator et al., 2020). Acetate can directly be converted to AcCoA by acetyl-CoA synthetase with ATP as a co-factor (Bator et al., 2020). Formate is not a carbon source as such for the microorganism. Instead, its metabolization into CO_2 produces NADH and, thus, can balance the energy demand of the cell (Zobel et al., 2017).

Methyl ketones are synthesized in the fatty acid metabolism, and the main precursor for this pathway is AcCoA. Hence, generally, the closer one substrate is in the map to the metabolite AcCoA, the easier the conversion to methyl ketones. In other words, less conversion steps with potential carbon or energy losses are necessary to form methyl ketones. Following this rule of thumb, ethanol and especially acetate are the most promising co-substrates. The FBA and the DoR results, however, ranked acetate lower. For ethylene glycol, despite its high DoR, the metabolic map supports the FBA results by showing that ethylene glycol can enter the GLX shunt instead of producing AcCoA.

We conclude that co-feeding can contribute to improving the yield of methyl ketones. Therein, ethanol is the most promising co-substrate, followed by glycerol. Ethylene glycol was shown to improve the methyl ketone yield less than expected from its high DoR. To finally evaluate the performance of acetate, laboratory experiments are necessary.

Ethanol Achieves the Highest Reported Yield in Shake Flask Cultivation

Prior to more detailed shake flask cultivations, the growth behavior of *P. taiwanensis* Δ6 pProd with the different co-fed carbon sources was investigated *in vivo* by online measurement of biomass formation in BioLector experiments. This cultivation showed substrate inhibition in the case of formate and acetate as a co-substrate (Supplementary Fig. A1). According to the FBA-based assessment of the co-substrates, ethanol was considered to be the most promising candidate for further evaluation in shake flask cultivations. The applied MSM media was developed to support cultivations with 10 g L^{-1} of glucose as a carbon source in shake flasks. To have the co-fed cultivations comparable to that, the same total molar amount of carbon was applied. A carbon ratio of two C-mol ethanol (2.4 g L^{-1}) to one C-mol glucose (8 g L^{-1}) was tested, and biomass growth, carbon source uptake, and methyl ketone formation was measured. Note that *P. taiwanensis* VLB120 produces minor amounts of gluconate as the only by-product. After glucose depletion, it also takes up gluconate. Accordingly, there are no side products to be taken into account for the overall assessment of these cultivations. Figure 3 shows the result of the shake flask cultivation.

Glucose and ethanol were taken up simultaneously, while the rate of glucose uptake occurred to be 1.44 ± 0.13 mmol g_{CDW}^{-1} hr^{-1}, higher than the rate of ethanol uptake of 1.05 ± 0.02 mmol g_{CDW}^{-1} hr^{-1}. After complete carbon source depletion after 24 hr, 0.84 ± 0.004 g L_{aq}^{-1} of methyl ketones were produced, corresponding to a yield of 84 mg_{MK} $g_{substrate}^{-1}$. Opposed to that, cultivations under the same conditions with only glucose as a carbon source had an average yield of 58 mg_{MK} $g_{substrate}^{-1}$. These cultivations show that glucose and ethanol are co-consumed without any diauxic behavior, with a higher uptake rate for ethanol. This indicates that, regarding biomass growth, glucose is the preferred substrate of the production host. However, by applying ethanol as a co-substrate, increased product concentrations and yields compared to glucose as a single substrate can be achieved. Biomass

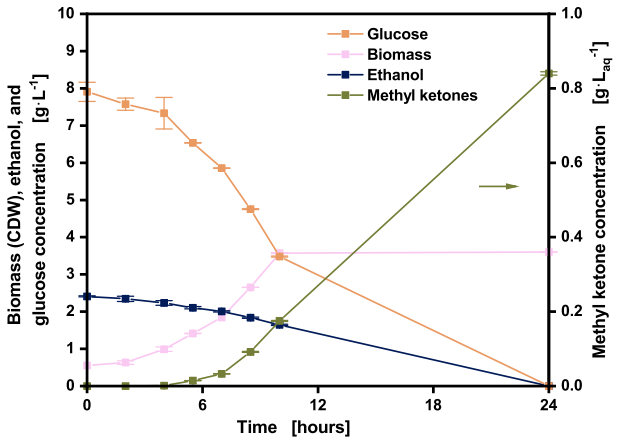

Fig. 3. Concentration of biomass, ethanol, glucose, and methyl ketones in a co-fed shake flask cultivation with *P. taiwanensis* Δ6 pProd. The C-molar ratios were one part glucose to two parts ethanol. The results are shown as the average of three experiments, and the error bar represents the standard deviation from these biological replicates.

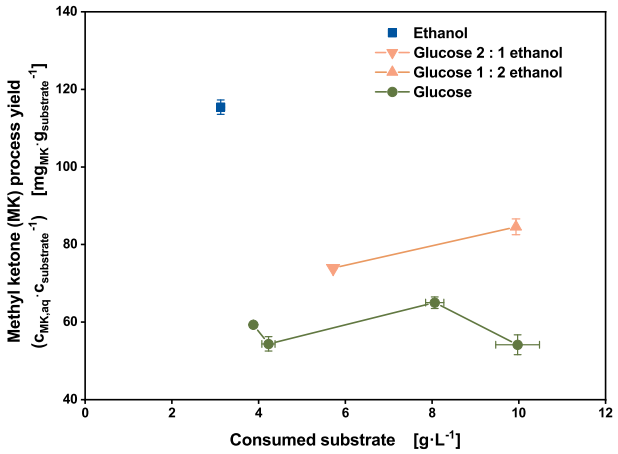

Fig. 4. Methyl ketone yield of (co-fed) shake flask cultivation after 24 hr and corresponding concentration of the carbon source. Glucose and ethanol were added in C-molar ratios of two parts glucose to one part ethanol (downward facing triangle) and one part glucose to two parts ethanol (upward facing triangle). Data are shown as the average and standard deviation of three biological replicates.

concentration increases exponentially and appears to stop after around 10 hr, which might, however, be due to nonoptimal sampling time points. Presumably, the strain was still in the exponential phase after 10 hr and grew around 1 or 2 hr more. According to our experimental experience, after reaching the stationary phase, the biomass decreases slightly. Presumably, the biomass concentration was higher than 3.6 g L^{-1} in the time when no sample was taken from the shake flask. The majority of product formation happened in the second half of the cultivation, presumably after substrate depletion. This was also observed earlier in cultivations with *P. taiwanensis* Δ6 pProd for methyl ketone production. This can occur due to the rate-limiting spontaneous decarboxylation observed before (Goh et al., 2014; Nies et al., 2020). Potentially, the product concentration could have increased further after the 24 hr that were investigated.

After confirming the simultaneous consumption of ethanol and glucose using *P. taiwanensis* Δ6 pProd as a production host, different combinations of glucose and ethanol were tested and compared regarding product yield and final product titer (Fig. 4).

All samples were taken 24.0 or 25.5 hr after inoculation, presumably not corresponding to the highest product yield since product concentrations were still increasing at that time point. The highest yield was obtained by using pure ethanol as a substrate. In the cultivation with ethanol as the only substrate, 2.82 g L^{-1} of ethanol were converted to methyl ketones with a product yield of 115 mg_{MK} $g_{substrate}^{-1}$. By applying ethanol and glucose in C-molar ratios of 2:1 and 1:2, yields of 84.56 and 74 mg_{MK} $g_{substrate}^{-1}$ were observed. When only glucose was used, the yield varied between 54 and 66 mg_{MK} $g_{substrate}^{-1}$. Presumably, these variations derive from slightly different sampling time points. The higher the supplied amount of ethanol, the higher the yield of methyl ketones. This suits the findings of the FBA study. After 48 hr of cultivation, a methyl ketone yield of 154 mg_{MK} $g_{substrate}^{-1}$ was observed in a shake flask cultivation with single-fed ethanol (Supplementary Fig. A2). To our knowledge, this is the highest reported yield of methyl ketones in batch cultivations with *P. taiwanensis* VLB120 to date. Using genetically engineered *P. putida* KT2440, a methyl ketone yield of 169 mg_{MK} $g_{substrate}^{-1}$ was observed in batch cultivations with glucose and high-value amino acids as co-substrates (Dong et al., 2019). On glucose as a single carbon source, *P. taiwanensis* VLB120 Δ6 pProd was able to produce 101 ± 2 mg L^{-1} in batch cultivations (Nies et al., 2020). Approaches to produce methyl ketones from carbon sources other than glucose and glycerol (Yan et al., 2020) are, to the best of our knowledge, not published. However, ethanol conversion takes place at a reduced rate compared to glucose, and no high ethanol concentrations can be applied due to product toxicity. Thus, the final product concentration of 0.48 g L_{aq}^{-1} in the cultivation with ethanol is also lower than 0.84 g L_{aq}^{-1} that was achieved with glucose and ethanol.

The Comparison of Experimental Data and Simulations Furnishes Consistent Results

We compared the experimental results from the shake flask cultivation with FBA results. From the experiments, we concluded that FBA with the assumption of simultaneous metabolization of the substrates is a valid tool, as no diauxic growth was visible during cultivation. The aim of this comparison was threefold. First, the validity of the GEM iJN1463_MK Δ6 pProd should be investigated. Second, the laboratory analysis of biomass should be analyzed. Third, we wanted to see whether there was potential for further improvement of the methyl ketone yield.

In order to compare the results, experimental values were transformed into fluxes. The input to the FBA was set to the uptakes that were measured in the experiments.

In a first step, we conducted an FBA, where we set an input of 2.77 mmol g_{CDW}^{-1} hr^{-1} glucose, corresponding to the measured value. In the corresponding batch cultivation experiment, no methyl ketone production was induced. Hence, in the FBA, biomass production was set as objective function. The FBA returns a production of 0.27 hr^{-1}, which fits the measured value of 0.28 hr^{-1}. We conclude that the GEM iJN1463_MK Δ6 pProd is able to simulate the biomass production.

In a second step, we compared the results from the best performing methyl ketone production cultivation, as presented in Fig. 3, to FBA results. In the FBA, the uptake of ethanol was set to 1.05 mmol g_{CDW}^{-1} hr^{-1} and the uptake of glucose was set to 1.44 mmol g_{CDW}^{-1} hr^{-1}. We set the methyl ketone exchange reaction as objective function, with the following stoichiometry:

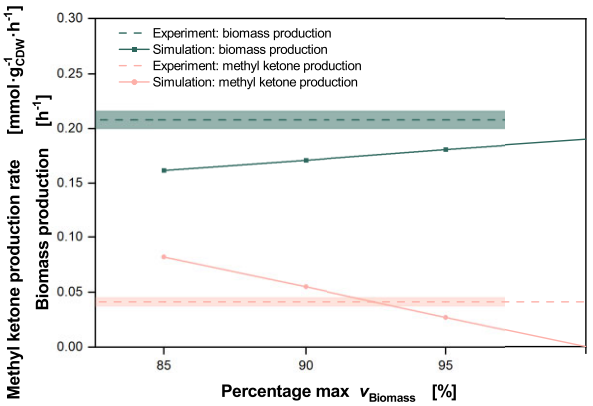

Fig. 5. Comparison of experimental biomass production and methyl ketone production with flux balance analysis (FBA) results. FBA conditions: The methyl ketone exchange reaction was set as objective function. The biomass threshold was varied from 85% to 100% of the maximal theoretical biomass production, that is, the flux of the biomass reaction $v_{Biomass}$. Glucose uptake was set to 1.44 mmol g_{CDW}^{-1} hr^{-1}, ethanol uptake was set to 1.05 mmol g_{CDW}^{-1} hr^{-1}. Cultivation conditions: 1 part C-mol glucose, 2 parts C-mol ethanol, $n = 300$ min^{-1}; $T = 30°C$; $V_{l,\ aq} = 50$ mL; $V_{l,\ org} = 12.5$ mL; $t = 24$ hr; $N = 3$; $c_{carbon} = 0.33$ C-mol. Errors were calculated with the jackknife method by Harris (1998).

$$1.00 \cdot \text{2-pentadecanone\_e} + 9.18 \cdot \text{8-pentadecen-2-one\_e}$$
$$+1.25 \cdot \text{10-heptadecen-2-one\_e} + 7.80 \cdot \text{2-tridecanone\_e}$$
$$+6.43 \cdot \text{6-tridecen-2-one\_e} + 5.66 \cdot \text{2-undecanone\_e} \rightarrow$$

that was determined from the measured ratio of congeners. The experimental methyl ketone production rate is 0.041 ± 0.004 mmol g_{CDW}^{-1} hr^{-1}. This value corresponds to 7.48% of the theoretical flux of methyl ketones when no threshold on biomass is set in the FBA. Next, in four different FBAs, we constrained biomass formation to find out which simulation fits the measured results. Figure 5 shows the comparison.

The methyl ketone production rate is a sum of all congener reaction fluxes. The experimental biomass growth is 0.208 ± 0.008 hr^{-1}. The simulated growth ranges from 0.162 hr^{-1} to 0.190 hr^{-1}, which corresponds to 85% to 100% of the theoretical biomass production. Hence, even the maximal theoretical biomass production does not reach the measured level of biomass. With the validation of the GEM beforehand, we conclude an experimental measurement error. When producing methyl ketones, the biomass was measured in a second, parallel flask, as the added organic solvent for *in situ* product extraction made simultaneous measurement of biomass and products in the same shake flask infeasible. We conclude that this laboratory analysis procedure needs to be revised.

When setting a threshold of 85% of the maximal theoretical biomass production, the simulated methyl ketone production is 0.082 mmol g_{CDW}^{-1} hr^{-1}. The production declines to zero when only biomass is produced at 100% of the theoretical biomass production. The intersection point with the experimental value is at 92.5% biomass threshold. In other words, the FBA predicts the same methyl ketone production as the experimental value when setting a threshold on biomass of 92.5% of the maximal theoretical biomass production. The threshold corresponds to a growth rate of 0.18 hr^{-1}.

We conclude from the comparative study that the FBA with the GEM iJN1463_MK Δ6 pProd was able to correctly predict the biomass production. Moreover, we found the potential to improve

the laboratory analysis of biomass measurement during methyl ketone production as the measured value was too high. Lastly, we conclude from the high threshold of 92.5% of the maximal biomass production that there is still room for improvement in the methyl ketone production. More carbon atoms could be used for methyl ketone production instead of being incorporated into biomass formation.

Conclusion

We investigated a co-feeding strategy for the production of methyl ketones with *P. taiwanensis* VLB120 Δ6 pProd. We presented an updated GEM, namely, iJN1463_MK, for metabolic modeling of *P. taiwanensis* VLB120 and performed FBA for five different co-substrates. Together with information on the DoR of the substrate as well as the uptake metabolism of each substrate from literature, ethanol was ranked highest. Ethanol has the additional advantage that it is a low-cost, high-volume product of many industrial processes. Sustainable industrial-scale production is enabled by the conversion of side and waste streams such as lignocellulosic biomass or biogas (Broda et al., 2022). Finetuning of the GEM, that is, revising the uptake metabolism of the co-substrates, might further increase its predictive potential. In batch cultivation, methyl ketone yields were highest on ethanol as sole carbon source. However, high concentrations of ethanol are toxic to the cell (Heipieper & Bont, 1994). Consequently, co-feeding with glucose has achieved higher product concentrations, while no diauxic metabolism was observed. In order to further increase the product concentrations, the cellular tolerance to ethanol should be increased by adaptive laboratory evolution (ALE) approaches. Moreover, fed-batch fermentation can help exploiting the full potential. A first growth phase makes the cells more robust to high ethanol concentrations, which makes it possible to increase the concentration of the carbon source. Alternatively, methyl ketone production in resting cells may be attractive, thereby uncoupling growth and product synthesis. Furthermore, the optimal ethanol-to-glucose ratio should be investigated next. When comparing the experimental with computational results, we have observed that there is still potential for improvement in the product yield because many of the carbon atoms are still metabolized to biomass. Genetic modification might further increase the yield. Again, a combined approach of metabolic modeling and experimental data is helpful. Gene knockouts can be predicted *in silico* by suitable bilevel optimization formulations (Burgard et al., 2003; Tepper and Shlomi, 2010) and can reduce the effort of subsequent *in vitro* experiments.

Supplementary Material

Supplementary material is available online at *JIMB* (*www.academic.oup.com/jimb*).

Funding

This work was supported by the Deutsche Forschungsgemeinschaft (DFG, German Research Foundation) under Germany's Excellence Strategy—Cluster of Excellence 2186 "The Fuel Science Center"—ID: 390919832 and by the Ministry of Culture and by the Ministry of Culture and Science within the framework of the "NRW Strategieprojekt BioSC" (No. 313/323400-002 13).

Author Contributions

A.L.Z. designed the computations and guided the network adaptations. C.G. designed the laboratory experiments. L.P. performed the network adaptations, the computational work, and experimental laboratory work under the supervision of A.L.Z. and C.G. A.L.Z., C.G., and L.P. visualized, analyzed, and discussed the data. A.L.Z. and C.G. wrote the manuscript draft. A.M. and L.M.B. conceptualized the project, discussed the data and reviewed the draft. All authors read and approved the final manuscript.

Conflict of Interest

No conflicts to declare.

Data Availability

The data underlying this article are available in our GitLab repository "Co-feeding enhances the yield of methyl ketones" at https://git.rwth-aachen.de/avt-svt/public/methylketones_cofeeding, cf. Ziegler et al. (2023).

References

Balakrishnan, M., Arab, G. E., Kunbargi, O. B., Gokhale, A. A., Grippo, A. M., Toste, F. D., & Bell, A. T. (2016). Production of renewable lubricants via self-condensation of methyl ketones. *Green Chemistry*, 18(12), 3577–3581. https://doi.org/10.1039/C6GC00579A

Bator, I., Karmainski, T., Tiso, T., & Blank, L. M. (2020). Killing two birds with one stone—strain engineering facilitates the development of a unique rhamnolipid production process. *Frontiers in Bioengineering and Biotechnology*, 8, 899. https://doi.org/10.3389/fbioe.2020.00899

Bengelsdorf, F. R. & Dürre, P. (2017). Gas fermentation for commodity chemicals and fuels. *Microbial Biotechnology*, 10(5), 1167–1170. https://doi.org/10.1111/1751-7915.12763

Broda, M., Yelle, D. J., & Serwanska, K. (2022). Bioethanol production from lignocellulosic biomass-challenges and solutions. *Molecules*, 27(24), 8717. https://doi.org/10.3390/molecules27248717

Burgard, A. P., Pharkya, P., & Maranas, C. D. (2003). Optknock: A bilevel programming framework for identifying gene knockout strategies for microbial strain optimization. *Biotechnology and Bioengineering*, 84(6), 647–657. https://doi.org/10.1002/bit.10803

Chmiel, H., Takors, R., & Weuster-Botz, D. (Eds). (2018). *Bioprozesstechnik* (4th ed.). Springer. https://doi.org/10.1007/978-3-662-54042-8

Cotton, C. A. R., Claassens, N. J., Benito-Vaquerizo, S., & Bar-Even, A. (2020). Renewable methanol and formate as microbial feedstocks. *Current Opinion in Biotechnology*, 62, 168–180. https://doi.org/10.1016/j.copbio.2019.10.002

Dong, J., Chen, Y., Benites, V. T., Baidoo, E. E. K., Petzold, C. J., Beller, H. R., Eudes, A., Scheller, H. V., Adams, P. D., Mukhopadhyay, A., Simmons, B. A., & Singer, S. W. (2019). Methyl ketone production by *Pseudomonas putida* is enhanced by plant-derived amino acids. *Biotechnology and Bioengineering*, 116(8), 1909–1922. https://doi.org/10.1002/bit.26995

Ebert, B. E., Kurth, F., Grund, M., Blank, L. M., & Schmid, A. (2011). Response of *Pseudomonas putida* KT2440 to increased NADH and ATP demand. *Applied and Environmental Microbiology*, 77(18), 6597–6605. https://doi.org/10.1128/AEM.05588-11

Ebrahim, A., Lerman, J. A., Palsson, B. O., & Hyduke, D. R. (2013). COBRApy: Constraints-based reconstruction and analysis for python. *BMC Systems Biology*, 7(1), 74. https://doi.org/10.1186/1752-0509-7-74

Goh, E. B., Baidoo, E. E., Keasling, J. D., & Beller, H. R. (2012). Engineering of bacterial methyl ketone synthesis for biofuels. *Applied and Environmental Microbiology*, 78(1), 70–80. https://doi.org/10.1128/AEM.06785-11

Goh, E. B., Baidoo, E. E. K., Burd, H., Lee, T. S., Keasling, J. D., & Beller, H. R. (2014). Substantial improvements in methyl ketone production in *E. coli* and insights on the pathway from in vitro studies. *Metabolic Engineering*, 26, 67–76. https://doi.org/10.1016/j.ymben.2014.09.003

Goh, E. B., Chen, Y., Petzold, C. J., Keasling, J. D., & Beller, H. R. (2018). Improving methyl ketone production in *Escherichia coli* by heterologous expression of NADH-dependent FabG. *Biotechnology and Bioengineering*, 115(5), 1161–1172. https://doi.org/10.1002/bit.26558

Gurobi Optimization, LLC. (2023). *Gurobi Optimizer Reference Manual*. https://www.gurobi.com

Harris, D. C. (1998). Nonlinear least-squares curve fitting with Microsoft Excel solver. *Journal of Chemical Education*, 75(1), 119. https://doi.org/10.1021/ed075p119

Harrison, K. W. & Harvey, B. G. (2018). High cetane renewable diesel fuels prepared from bio-based methyl ketones and diols. *Sustainable Energy & Fuels*, 2(2), 367–371. https://doi.org/10.1039/c7se00415j

Hartmans, S., Smits, J. P., van der Werf, M. J., Volkering, F., & de Bont, J. A. (1989). Metabolism of styrene oxide and 2-phenylethanol in the styrene-degrading *Xanthobacter* strain 124x. *Applied and Environmental Microbiology*, 55(11), 2850–2855. https://doi.org/10.1128/aem.55.11.2850-2855.1989

Heijnen, J. J. & Roels, J. A. (1981). A macroscopic model describing yield and maintenance relationships in aerobic fermentation processes. *Biotechnology and Bioengineering*, 23(4), 739–763. https://doi.org/10.1002/bit.260230407

Heipieper, H. J. & de Bont, J. A. (1994). Adaptation of *Pseudomonas putida* S12 to ethanol and toluene at the level of fatty acid composition of membranes. *Applied and Environmental Microbiology*, 60(12), 4440–4444. https://doi.org/10.1128/aem.60.12.4440-4444.1994

Hollinshead, W., He, L., & Tang, Y. J. (2014). Biofuel production: An odyssey from metabolic engineering to fermentation scale-up. *Frontiers in Microbiology*, 5, 344. https://doi.org/10.3389/fmicb.2014.00344

Lang, K., Zierow, J., Buehler, K., & Schmid, A. (2014). Metabolic engineering of *Pseudomonas* sp. strain VLB120 as platform biocatalyst for the production of isobutyric acid and other secondary metabolites. *Microbial Cell Factories*, 13(1), 2. https://doi.org/10.1186/1475-2859-13-2

Lenzen, C., Wynands, B., Otto, M., Bolzenius, J., Mennicken, P., Blank, L. M., & Wierckx, N. (2019). High-yield production of 4-hydroxybenzoate from glucose or glycerol by an engineered *Pseudomonas taiwanensis* VLB120. *Frontiers in Bioengineering and Biotechnology*, 7, 130. https://doi.org/10.3389/fbioe.2019.00130

Li, W.-J., Jayakody, L. N., Franden, M. A., Wehrmann, M., Daun, T., Hauer, B., Blank, L. M., Beckham, G. T., Klebensberger, J., & Wierckx, N. (2019). Laboratory evolution reveals the metabolic and regulatory basis of ethylene glycol metabolism by *Pseudomonas putida* KT2440. *Environmental Microbiology*, 21 (10), 3669–3682. https://doi.org/10.1111/1462-2920.14703

Müller, J., MacEachran, D., Burd, H., Sathitsuksanoh, N., Bi, C., Yeh, Y. C., Lee, T. S., Hillson, N. J., Chhabra, S. R., Singer, S. W., & Beller, H. R. (2013). Engineering of *Ralstonia eutropha* H16 for autotrophic and heterotrophic production of methyl ketones. *Applied Environmental Microbiology*, 79(14), 4433–9. https://doi.org/10.1128/aem.00973-13

Nies, S. C., Alter, T. B., Nölting, S., Thiery, S., Phan, A. N. T., Drummen, N., Keasling, J. D., Blank, L. M., & Ebert, B. E. (2020). High titer methyl ketone production with tailored *Pseudomonas taiwanensis* VLB120. *Metabolic Engineering*, 62, 84–94. https://doi.org/10.1101/2020.06.02.125906

Nikel, P. I. & de Lorenzo, V. (2014). Robustness of *Pseudomonas putida* KT2440 as a host for ethanol biosynthesis. *New Biotechnology*, 31(6), 562–71. https://doi.org/10.1016/j.nbt.2014.02.006

Nogales, J., Gudmundsson, S., Duque, E., Ramos, J. L., & Palsson, B. O. (2017). Expanding the computable reactome in *Pseudomonas putida* reveals metabolic cycles providing robustness. *BioRxiv*, 139121. https://doi.org/10.1101/139121

Nogales, J., Mueller, J., Gudmundsson, S., Canalejo, F. J., Duque, E., Monk, J., Feist, A. M., Ramos, J. L., Niu, W., & Palsson, B. O. (2020). High-quality genome-scale metabolic modelling of *Pseudomonas putida* highlights its broad metabolic capabilities. *Environmental Microbiology*, 22(1), 255–269. https://doi.org/10.1111/1462-2920.14843

Orth, J. D., Thiele, I., & Palsson, B. Ø. (2010). What is flux balance analysis? *Nature Biotechnology*, 28(3), 245–248. https://doi.org/10.1038/nbt.1614

Park, J. O., Liu, N., Holinski, K. M., Emerson, D. F., Qiao, K., Woolston, B. M., Xu, J., Lazar, Z., Islam, M. A., Vidoudez, C., Girguis, P. R., & Stephanopoulos, G. (2019). Synergistic substrate cofeeding stimulates reductive metabolism. *Nature Metabolism*, 1(6), 643–651. https://doi.org/10.1038/s42255-019-0077-0

Poblete-Castro, I., Wittmann, C., & Nikel, P. I. (2020). Biochemistry, genetics and biotechnology of glycerol utilization in *Pseudomonas species*. *Microbial Biotechnology*, 13(1), 32–53. https://doi.org/10.1111/1751-7915.13400

Sivapuratharasan, V., Lenzen, C., Michel, C., Muthukrishnan, A. B., Jayaraman, G., & Blank, L. M. (2022). Metabolic engineering of *Pseudomonas taiwanensis* VLB120 for rhamnolipid biosynthesis from biomass-derived aromatics. *Metabolic Engineering Communications*, 15, e00202. https://doi.org/10.1016/j.mec.2022.e00202

Stephanopoulos, G., Aristidou, A. A., & Nielsen, J. (1998). *Metabolic engineering: Principles and methodologies*. Academic Press.

Sudarsan, S., Dethlefsen, S., Blank, L. M., Siemann-Herzberg, M., & Schmid, A. (2014). The functional structure of central carbon metabolism in *Pseudomonas putida* KT2440. *Applied and Environmental Microbiology*, 80(17), 5292–5303. https://doi.org/10.1128/AEM.01643-14

Sun, S., Ding, Y., Liu, M., Xian, M., & Zhao, G. (2020). Comparison of glucose, acetate and ethanol as carbon resource for production of poly(3-hydroxybutyrate) and other acetyl-CoA derivatives. *Frontiers in Bioengineering and Biotechnology*, 8, 833. https://doi.org/10.3389/fbioe.2020.00833.

Tepper, N. & Shlomi, T. (2010). Predicting metabolic engineering knockout strategies for chemical production: Accounting for competing pathways. *Bioinformatics*, 26(4), 536–543. https://doi.org/10.1093/bioinformatics/btp704.

Tiso, T., Narancic, T., Wei, R., Pollet, E., Beagan, N., Schröder, K., Honak, A., Jiang, M., Kenny, S. T., Wierckx, N., Perrin, R., Avérous, L., Zimmermann, W., O'Connor, K., & Blank, L. M. (2021). Towards bio-upcycling of polyethylene terephthalate. *Metabolic Engineering*, 66, 167–178. https://doi.org/10.1016/j.ymben.2021. 03.011

Ullmann, L., Phan, A. N. T., Kaplan, D. K. P., & Blank, L. M. (2021). *Ustilaginaceae biocatalyst* for co-metabolism of co(2)-derived substrates toward carbon-neutral itaconate production. *Journal of Fungi*, 7(2), 98. https://doi.org/10.3390/jof7020098

Varma, A. & Palsson, B. O. (1994). Stoichiometric flux balance models quantitatively predict growth and metabolic by-product

secretion in wild-type *Escherichia coli* W3110. *Applied and Environmental Microbiology*, 60(10), 3724–3731. https://doi.org/10.1128/aem.60.10.3724-3731.1994

Wordofa, G. G. & Kristensen, M. (2018). Tolerance and metabolic response of *Pseudomonas taiwanensis* VLB120 towards biomass hydrolysate-derived inhibitors. *Biotechnolology for Biofuels*, 11(1), 199. https://doi.org/10.1186/s13068-018-1192-y

Xu, Z., Pan, C., Li, X., Hao, N., Zhang, T., Gaffrey, M. J., Pu, Y., Cort, J. R., Ragauskas, A. J., Qian, W.-J., & Yang, B. (2021). Enhancement of polyhydroxyalkanoate production by co-feeding lignin derivatives with glycerol in *Pseudomonas putida* KT2440. *Biotechnology for Biofuels*, 14(1), 11. https://doi.org/10.1186/s13068-020-01861-2

Yan, Q., Simmons, T. R., Cordell, W. T., Hernández Lozada, N. J., Breckner, C. J., Chen, X., Jindra, M. A., & Pfleger, B. F. (2020). Metabolic engineering of β-oxidation to leverage thioesterases for production of 2-heptanone, 2nonanone and 2-undecanone. *Metabolic Engineering*, 61, 335–343. https://doi.org/10.1016/j.ymben.2020.05.008

Yang, J., Son, J. H., Kim, H., Cho, S., Na, J.-G., Yeon, Y. J., & Lee, J. (2019). Mevalonate production from ethanol by direct conversion through acetyl-CoA using recombinant *Pseudomonas putida*, a novel biocatalyst for terpenoid production. *Microbial Cell Factories*, 18(1), 168. https://doi.org/10.1186/s12934-019-1213-y

Ziegler, A. L., Grütering, C., Poduschnick, L., Mitsos, A., & Blank, L. M. (2023). *Open-source dataset: Co-feeding enhances the yield of methyl ketones*. https://git.rwth-aachen.de/avt-svt/public/methylketones_cofeeding.

Zobel, S., Kuepper, J., Ebert, B., Wierckx, N., & Blank, L. M. (2017). Metabolic response of *Pseudomonas putida* to increased NADH regeneration rates. *Engineering in Life Sciences*, 17(1), 47–57. https://doi.org/10.1002/elsc.201600072

Zu, S. N. K., Liu, S., Gerlach, E. S., Mojadedi, W., & Sund, C. J. (2021). Co-feeding glucose with either gluconate or galacturonate during clostridial fermentations provides metabolic fine-tuning capabilities. *Scientific Reports*, 11(1), 29. https://doi.org/10.1038/s41598-020-76761

Received: April 12, 2023. **Accepted:** September 11, 2023